

## 6-DOF Localization for a Mobile Robot using Outdoor 3D Voxel Maps

Taro Suzuki, Mitsunori Kitamura, Yoshiharu Amano and Takumi Hashizume

**Abstract**— This paper describes outdoor localization for a mobile robot using a laser scanner and a three-dimensional (3D) voxel map that is based on outdoor point clouds. A mobile mapping system (MMS) measures outdoor 3D point clouds easily and precisely. The complete 6D state of a mobile robot is estimated by combining dead reckoning and the 3D voxel map. The 2D position and orientation are extended to 3D by using the 3D voxel map and by assuming that the mobile robot remains in continuous contact with the road surface. Our approach applies a particle filter to correct position errors in the laser measurement model for a 3D point cloud space. Field experiments were performed to evaluate the accuracy of our proposed method. Our results confirmed that it is possible to achieve a localization precision of 0.2 m (RMS) using our proposed method.

### I. INTRODUCTION

A large number of studies have been conducted on methods that are used to estimate the position of mobile robots [1–4]; these methods are mainly probabilistic approaches that are used to estimate the position of mobile robots by matching sensor measurements to existing map data. Most of these studies adopt dead reckoning (DR) with encoders and gyroscopes for 2D estimations of position and orientation in 2D environmental maps.

On the other hand, recent developments in intelligent transportation system (ITS) related technologies have actively promoted the increased application of autonomous mobile systems in outdoor environments, such as unmanned construction systems by autonomous machinery and automatic vehicle navigation.

Unlike indoor environments, which generally have smooth or even surfaces, outdoor environments tend to be uneven, which prevents outdoor environments from being assumed to be 2D planes. Precise movement in outdoor environments thus requires the estimation of the position and attitude with six degrees of freedom (DOF).

A global positioning system/inertial navigation system (GPS/INS) is conventionally used to estimate the position and attitude of mobile robots in outdoor environments [5–7]. However, high-precision estimation by GPS/INS navigation requires very expensive sensors, such as dual-frequency GPS

receivers and ring laser gyroscopes; it is inconvenient to use such expensive sensors when cost is a consideration. Moreover, the accuracy of GPS positioning is impaired in urban canyons or leafy environments, which compels us to realize high-precision localization in outdoor environments with simple sensor configurations.

Recent developments in measuring technologies using lasers have promoted 3D measurements for mapping outdoor environments. In particular, mobile mapping systems (MMS) for 3D measurements of outdoor environments can acquire wide-ranging 3D outdoor point cloud data with high precision [8–10]. In spite of readily available outdoor 3D measurements, little research appears to have been conducted on applying 3D point cloud data to mobile robots or determining what mapping is required for such an application. Based on these circumstances, developments of autonomous mobile technologies using acquired 3D data of outdoor environments are in demand

In this study, we developed a method to estimate the 6-DOF position and attitude of mobile robots in outdoor environments with high precision—a few tens of centimeters to one degree—using a simple sensor configuration applied in indoor environments; we used 3D mapping based on 3D point cloud data acquired by MMS with high-precision sensors. The developed method consists of the following two phases: 3D mapping with MMS for mobile robots and constructing simple configurations to estimate the 6-DOF position and attitude using 3D maps.

In 3D mapping, maps are generated to enable mobile robots to use the measured 3D point cloud data. When estimating the position using such 3D maps, we can estimate position in outdoor environments with a precision of a few tens of centimeters by using particle filters to integrate 3D maps without the use of GPS; instead, we use DR by applying a sensor configuration with a one-axis gyroscope and encoder and laser-scanner data. We estimated the 6-DOF position and attitude using a minimum sensor configuration with DR and a laser scanner by developing a method to extend the 2D position and orientation into 3D by using 3D maps.

### II. RELATED WORKS AND ISSUES

Mobile robot position and attitude in outdoor environments is typically estimated using GPS/INS navigation based on the extensively studied extended Kalman filter (EKF). In the Defense Advanced Research Projects Agency (DARPA) Grand/Urban Challenge involving driverless outdoor vehicle races, most teams use GPS/INS navigation. In 2005, the Stanford University Racing Team achieved autonomous

Manuscript received February 28, 2010. This work was supported in part by the Research Fellowships of the Japan Society for the Promotion of Science for Young Scientists.

T. S. and M. K. are with the Graduate School of Science and Engineering, Waseda University, Tokyo, Japan (phone: +81-3-3203-4515; fax: +81-3-3203-3231; e-mail: taro@power.mech.waseda.ac.jp).

Y. A. and T. H. are with the Advanced Research Institute for Science and Engineering, Waseda University, Tokyo, Japan (hasizume@waseda.jp, yoshiha@waseda.jp).

running for over 200 km [7].

Our proposal to estimate positions in outdoor environments using a simple sensor configuration instead of GPS involves a 2D laser scanner and camera in environment recognition. The proposed method is largely divided into the following two categories: a method for simultaneous mapping and estimation of positions as represented by SLAM (Simultaneous Localization and Mapping); and a method to estimate positions by matching existing maps and sensor data.

The researches on the former method of SLAM in outdoor environments include 3D mapping with laser scanners and 6-DOF localization by Lingermann and Nuechter [11, 12] and localization with monocular cameras by Davison [13].

They have succeeded in localization in outdoor environments without using maps. In estimating positions by SLAM, however, high-precision estimations of position and attitude requires repeated observation (loop closure) at the same points during run; run routes will have great effects on precision, making it difficult to maintain precision of localization.

On the other hand, estimating position using existing environmental maps includes matching such as iterative closest point (ICP) algorithm [3, 17, 18] and particle filters [2, 4, 14, 15]. Monte Carlo localization (MCL), which matches maps and environmental recognition sensor data through particle filters, has been used in indoor environment localization [2] [14]. Researches on MCL in outdoor environments include research by Rainer [15], similar to our proposal. They proposed estimating position and attitude of mobile robots in outdoor environment using multilevel surface (MLS) maps. Related issues are how to prepare high-precision 3D outdoor mapping and estimate 6-DOF position and attitude in an undulating outdoor environment.

In this paper, we propose 3D voxel maps using 3D point cloud data acquired by MMS and propose estimating 6-DOF position and attitude from the position of a mobile robot's tires. We confirmed the precision of our proposal by comparing localization results from GPS/INS navigation.

### III. PROPOSAL OVERVIEW

The proposed method to estimate position using environmental 3D point clouds is consists of (1) 3D mapping with MMS and (2) localization of mobile robots using these prepared maps. Fig. 1 shows the localization algorithm flow with a particle filter using 3D environment maps. This algorithm requires (1) 3D environment maps based on MMS measurement and (2) a mobile robot with a DR sensor configuration with an encoder, a 1-axis gyroscope, and an environment-recognition by one laser range finder (LRF).

The algorithm is executed as follows:

(i) State vectors of particles are 2D positions  $x$ ,  $y$  and orientation (yaw angle)  $\psi$ . Probabilistic models of mobile robots are made using the encoder on the mobile robot drive wheel and 1-axis gyroscope for DR, calculating position and orientation and particle distribution.

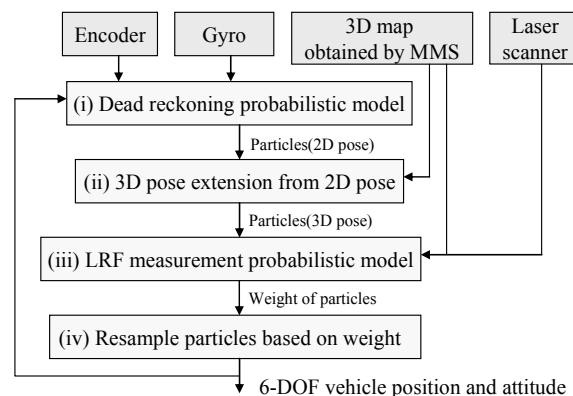


Fig. 1 Flowchart of localization using 3D point clouds.

(ii) The mobile robot altitude  $z$ , roll angle  $\theta$ , and pitch angle  $\phi$  are then estimated from the redistributed particles assuming that all robot tires are in constant contact with the road surface.

(iii) The LRF measurement is converted to 3D mapping coordinates based on the acquired 6-DOF position and attitude to calculate the likelihood of each particle through matching to 3D maps.

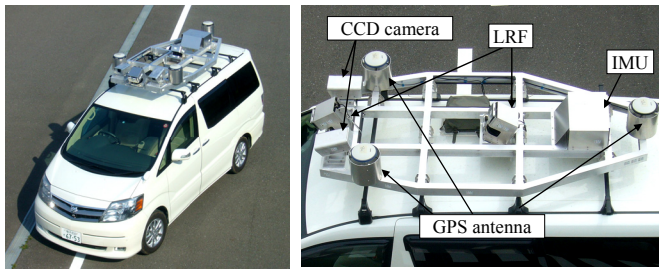
(iv) Particles are resampled on the basis of the likelihood thus acquired, and the average position and attitude of the resampled particles are taken to denote the final position and attitude of the mobile robot.

In the sections that follow, Section IV discusses 3D environment mapping based on 3D outdoor point cloud data acquired from MMS measurements, Section V extends the 3D position and attitude from the 2D position and orientation, Section VI calculates the likelihood using 3D maps with particle filters, and Section VII evaluates the precision of our proposed method for estimating the position and attitude through experiments in actual environments. Section VIII presents our conclusions.

### IV. 3D MAPPING

Fig. 2 shows the MMS and sensor configurations. MMS uses carrier-phase D-GPS and a fiber optic gyroscope (FOG) to measure the MMS position and attitude. In addition, we use a GPS-gyro/inertial measurement unit (IMU) to combine estimations of position and attitude; the attitude estimated by GPS-gyro using three GPS antennas are combined together through EKF [9].

Two LRFs (LMS291, SICK Inc.) used for 3D measurement permit distance measurements with a cataloged precision of  $\pm 35$  mm; they provide degree-by-degree scanning for a range  $180^\circ$ . Environmental 3D point cloud data are acquired by synchronizing sensors based on GPS time information and reconstructed using the position and attitude of the MMS and the measurement data acquired from the LRF. This system, which allows high-precision estimation of the position and attitude in urban or leafy environments, or where satellite transmissions are likely to be cut off, has proved capable of taking precise 3D measurements of outdoor environments over a broad range with a standard deviation ( $1\sigma$ ) of 10 cm [9].



(a) MMS (b) Sensor configuration  
Fig. 2 Mobile mapping system (MMS).

Fig. 3 shows 3D scene reconstruction that uses MMS to easily acquire high-precision 3D point cloud data for a broad range of outdoor environments.

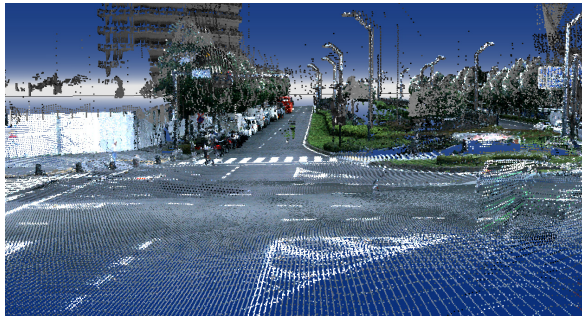


Fig. 3 3D scene reconstruction using MMS.

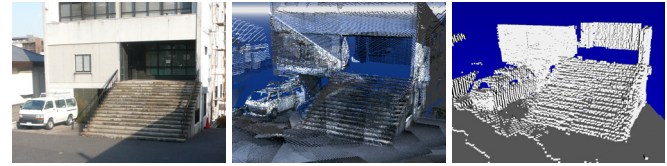
Applying such 3D point cloud data for the localization of autonomous mobile robots raises the following issues:

- (1) Computers require a huge amount of memory to process such large quantities of data, and the random time-sequenced data configuration adversely affects retrieval performance.
- (2) 3D measurement resolution varies with measurement distance, resulting in nonuniformity in 3D space.

To handle these issues and enable an autonomous mobile robot to easily process 3D point cloud data acquired with MMS for localization purposes, we quantized 3D point clouds in voxel space for use in 3D environment maps. Data volume is reduced through uniformly quantizing and extracting only highly probabilistic points after the 3D point cloud data are voting-processed into voxel space. In these processes, the higher the voxel space resolutions, the more accurately 3D shapes are represented. However, this requires an extremely large amount of memory. Therefore, we quantized data into blocks of  $100 \text{ mm} \times 100 \text{ mm} \times 10 \text{ mm}$  in the  $x$ ,  $y$ , and  $z$  axis directions. We used higher resolution for the  $z$ -axis direction alone to accurately reproduce road surface shape and data on obstacles. Such 3D voxel point clouds present such a sparse 3D array that we compressed them into a sparse matrix for retention in the computer memory.

Fig. 4 shows voxel voting to generate 3D maps from 3D point clouds. Comparing (a) the photo of the environment and (b) 3D point clouds acquired using MMS shows that environments were accurately represented by the 3D point clouds. Fig. 4(c) shows a voxel model confirming that

environments were constructed with continuous resolution. For these environments, we created 3D voxel maps for experimental environments of  $100 \text{ mm} \times 100 \text{ mm}$ ; on average, four measurement points were included around the road surfaces. Compressing 3D voxel maps into a sparse matrix resulted in a size of 3 MB in  $100 \text{ m} \times 100 \text{ m}$  environment.



(a) Photo of environment (b) 3D point clouds (c) Voxel model  
Fig. 4 Voxel voting for generating 3D maps.

## V. EXTENSION OF 2D POSITION AND ORIENTATION INTO 3D

### A. Algorithm

The estimated position and attitude of mobile robots are often represented by 2D plane coordinates. This approximation enables the robots to calculate their self-position with an encoder by measuring wheel revolutions and using a one-axis gyroscope measure angular rate. However, operating mobile robots in outdoor environments means that the position and attitude of mobile robots vary widely with the conditions of road surfaces, where there are lots of ups and downs or steps; in particular, the attitudes of robots in terms of roll and pitch angles significantly affect the distance information acquired by an LRF. Therefore, 3D position and attitude information are critical for matching LRF measurement results to outdoor maps.

Unlike indoor environments, position and attitude information outdoors must be represented by 6-DOF information in 3D space: position  $(x, y, z)$  in robot coordinates relative to world coordinates, roll angle  $\varphi$ , pitch angle  $\theta$ , and yaw angle  $\psi$ . Encoders and one-axis gyroscopes only estimate data on the  $(x, y)$  position and yaw angle  $\psi$  for the orientation, but not the three remaining variables, i.e.,  $z$ ,  $\varphi$ , and  $\theta$ . Therefore, we propose extending coordinates  $(x, y, \psi)$  on the 2D plane to coordinates  $(x, y, z, \varphi, \theta, \psi)$  in 3D space using the above 3D voxel environment maps.

The unknown robot altitude  $z$  is acquired by calculating the 2D position  $(x_{\text{tire}}, y_{\text{tire}})$  of tires from the robot position  $(x, y)$  acquired by DR. Assuming that the robot continuously touches the road surfaces, the altitude  $z_{\text{tire}}$  on the 3D voxel map directly beneath the tire positions  $(x_{\text{tire}}, y_{\text{tire}})$  is determined as the tire altitude in 3D space. The robot altitude  $z$  is calculated by averaging the tire altitude  $z_{\text{tire}}$  in 3D space.

Next, we acquire the rotation matrix  $R$  from the world coordinates to the robot coordinates to determine the robot roll angle  $\varphi$  and pitch angle  $\theta$ . Road surfaces touched by the robot are first defined by tire coordinates  $(x_{\text{tire}}, y_{\text{tire}}, z_{\text{tire}})$  from 3D voxel maps; the attitude is then calculated from normal vector  $n_m$  of the road surface. Fig. 5 shows the 3D rotation matrix estimated from the normal vector.

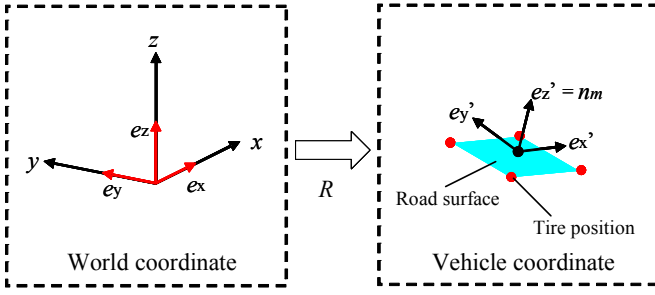


Fig. 5 3D rotation matrix determination from normal vector.

With the  $x$ -,  $y$ -, and  $z$ -axis unit vectors in world coordinates expressed by  $e_x = (1, 0, 0)$ ,  $e_y = (0, 1, 0)$ , and  $e_z = (0, 0, 1)$ ,  $e_x$ ,  $e_y$ , and  $e_z$  are defined as converted to  $e_x'$ ,  $e_y'$ , and  $e_z'$  by rotation matrix  $R$  from world coordinates to vehicle coordinates as follows:

$$R = \begin{pmatrix} r_{11} & r_{12} & r_{13} \\ r_{21} & r_{22} & r_{23} \\ r_{31} & r_{32} & r_{33} \end{pmatrix} [e_x, e_y, e_z] = [e_x', e_y', e_z'] \quad (1)$$

As Fig. 5 shows, the unit vector  $e_z'$  after conversion by rotation matrix  $R$  is identical to the normal vector  $n_m$  of the mobile robot.

In this study, we used mobile robots with four wheels, for which the normal vector  $n_m$  is determined by averaging the normal vectors calculated from different tire combinations. Using the condition where the yaw angle  $\psi$  is known out of the three attitude angles  $\phi$ ,  $\theta$ ,  $\psi$ , the remaining  $e_x'$  and  $e_y'$  are acquired.  $e_x'$  is acquired by calculating the vector of unit vector  $e_y$  rotated by  $\psi$  around the  $z$ -axis in world coordinates, and the unit vector orthogonal to the plane is expressed by  $e_z'$ :

$$e_x' = \text{normalize} \left( R(Z, \psi) e_y \times e_z' \right) \quad (2)$$

where  $\text{normalize}$  denotes vectors normalization and  $R(Z, \psi)$  denotes the rotation by  $\psi$  around the  $Z$ -axis.  $e_y'$  is calculated using the  $e_x'$  and  $e_z'$  acquired from Eq. (2):

$$e_y' = \text{normalize} \left( e_z' \times e_x' \right) \quad (3)$$

The rotation matrix  $R$  from world coordinates to robot coordinates is acquired by substituting  $e_x'$  and  $e_y'$  and the known  $e_z'$  into Eq. (1). The attitude angles  $\phi$  and  $\theta$  are calculated by substituting  $R$  components into the following:

$$\phi = \tan^{-1} \left( \frac{r_{32}}{r_{33}} \right) \quad (4)$$

$$\theta = \sin^{-1}(-r_{31}) \quad (5)$$

Based on the above, the 2D estimation of the position and orientation using an encoder and gyroscope can be extended into a 3D attitude by using 3D voxel environment maps.

## B. Validation of Precision in Extension of Position

We conducted experiments to evaluate the precision of our proposal in calculating altitude  $z$ , roll angle  $\phi$ , and pitch angle  $\theta$  for attitude information, using environmental 3D voxel maps. In evaluating precision, we used reference information on altitude and attitude consisting of three-axis position and attitude calculated using GPS-gyroscope of MMS and a three-axis FOG used for 3D mapping. Precision was evaluated as follows:

For true values in precision evaluation, we take 6-DOF position and attitude  $(x_{ref}, y_{ref}, z_{ref}, \phi_{ref}, \theta_{ref}, \psi_{ref})$  calculated using the MMS GPS and the three-axis FOG. Based on 2D position and orientation  $(x_{ref}, y_{ref}, \psi_{ref})$  data on 2D planes, we compared data on 3D position and attitude  $(z_{est}, \phi_{est}, \theta_{est})$  and  $(z_{ref}, \phi_{ref}, \theta_{ref})$  acquired from calculation using 3D voxel maps as we proposed. Fig. 6 shows estimation results for altitude  $z_{est}$  and attitude angles  $\phi_{est}$ ,  $\theta_{est}$ . Evaluation experiments showed that standard deviation ( $\sigma$ ) of altitude  $z$  is 0.0507 m, standard deviation of attitude angle  $\phi$  is 0.4050 deg, and standard deviation of attitude angle  $\theta$  is 0.4083 deg. The quantization error of the voxel 3D map and the effect of the suspensions of the vehicle can be thought to cause the residual error.

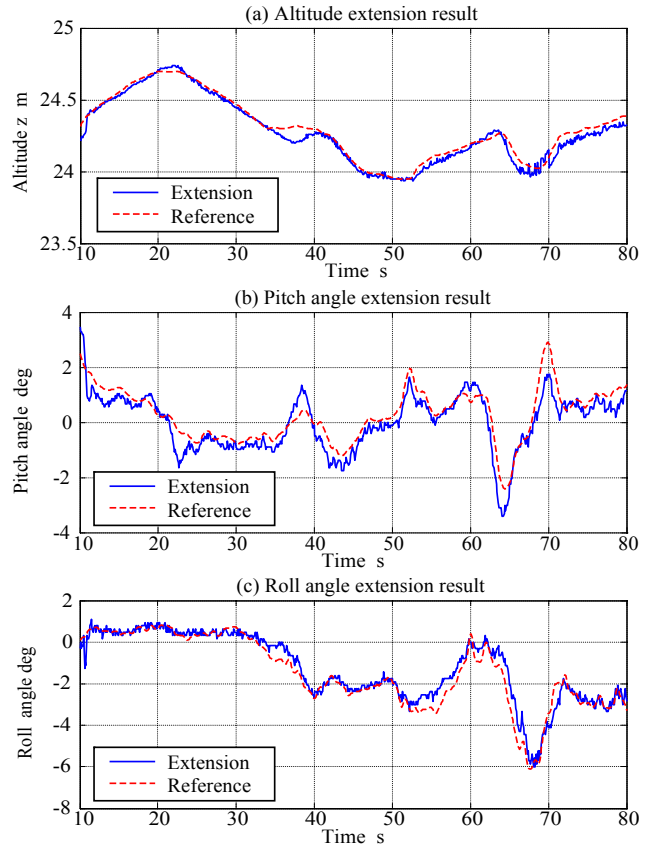


Fig. 6 3D position and attitude extension results.

## VI. POSITION ESTIMATION OF THROUGH PARTICLE FILTERS

In the preceding section, we demonstrated that once the 2D position and orientation  $(x, y, \psi)$  are acquired, they can be extended to 3D position and attitude using 3D voxel maps.

With the state vector at given time  $t$  expressed by  $x_t = (x, y, \psi)$ , the likelihood of state vector  $x_t$  is acquired by matching LRF measurement results to 3D voxel environment maps. This is combined with DR through particle filters to acquire the determined state vector  $x_t$ .

Using the time-sequential set of LRF measurement results until time  $t$  expressed by  $z_{1:t}$  and measurement results from sensors for DR by the odometer and gyroscope expressed by  $u_{0:t-1}$ , the probability  $p(x_t|z_{1:t}, u_{0:t-1})$  of state vector  $x_t$  of the mobile robot at the given time  $t$  is formulated by the recurrence formula Eq. (6), where  $p(z_t|x_t)$  is the probability distribution of the measurement model and  $p(x_t|u_{t-1}, x_{t-1})$  is the probability distribution of the motion model.

$$p(x_t|z_{1:t}, u_{0:t-1}) = \eta p(z_t|x_t) \int p(x_t|u_{t-1}, x_{t-1}) p(x_{t-1}) dx_{t-1} \quad (6)$$

where  $\eta$  is the coefficient for normalization. As shown in Eq. (6), the measurement results  $z_{1:t}$  from LRF and probabilities  $p(x_t|z_{1:t}, u_{0:t-1})$  of the position and attitude, as estimated on sensor-measurement results  $u_{0:t-1}$  for DR are expressed by the motion model  $p(x_t|u_{t-1}, x_{t-1})$  of the robot in predictive steps and sensor-measurement model  $p(z_t|x_t)$  in observatory steps. Particle filters approximate the probabilities  $p(x_t|z_{1:t}, u_{0:t-1})$  of the position and attitude, which are estimated by approximating the above probability-distributions with particle sets. When applying the motion model  $p(x_t|u_{t-1}, x_{t-1})$  of the mobile robot by DR to particles, the robot position and attitude are calculated from revolutions of the rotary encoder in tires and changes in attitude angles in the gyroscope. These models are produced by providing random numbers to rotary encoder travel and changes in gyroscope attitude angles for normal distributions, with the errors in the respective sensors taken into account. With the state vector of the  $i$ th particle at time  $t$  expressed by  $x_{t,i} = (x_{t,i}, y_{t,i}, \psi_{t,i})$ , encoder travel from time  $t-1$  until time  $t$ , by  $\Delta v_t$  and changes in yaw angles  $\psi$  as measured by the gyroscope by  $\Delta \psi$ , the movement of particles by DR are expressed by Eq. (7):

$$x_{t,i} = x_{t-1,i} + \begin{bmatrix} R(\psi_{t-1,i} + \Delta \psi + w_{\psi,t,i}) (\Delta v_t + w_{v,t,i}) \\ \Delta \psi + w_{\psi,t,i} \end{bmatrix} \quad (7)$$

$R(\cdot)$  is the 2D rotation matrix or rotation by angle  $(\cdot)$ ,  $w_{v,t,i}$  is the encoder distance error, and  $w_{\psi,t,i}$  is the gyroscope angle error defined as follows:

$$p(w_v) = \frac{1}{\sqrt{2\pi\sigma_{wv}^2}} \exp\left\{-\frac{1}{2\sigma_{wv}^2} w_v^2\right\} \quad (8)$$

$$p(w_\psi) = \frac{1}{\sqrt{2\pi\sigma_{w\psi}^2}} \exp\left\{-\frac{1}{2\sigma_{w\psi}^2} w_\psi^2\right\} \quad (9)$$

For the dispersion of errors  $\sigma_{wv}$  in the encoder and the

dispersion of angle errors  $\sigma_{w\psi}$  in the gyroscope, we used values from experiments based on sensor specifications. Eqs (8) and (9) use encoder and gyroscope measurement input to approximate the probabilistic prediction of state vectors in the following time steps using particles.

Next, when calculating the likelihood using an LRF measurement model, this model should be designed so that the likelihood of state vector  $x_t$  becomes greatest when the ambient distance data  $z_t$  measured using the LRF coincides with the 3D point cloud data of environments measured in advance. We define the measurement probabilistic model  $p(z_t|x_t)$  with the LRF by approximate expressions such as Eq. (10):

$$p(z_t|x_t) \approx \frac{1}{\sqrt{2\pi\sigma^2}} \exp\left(-\frac{d(\text{map}, z_t, x_t)^2}{2\sigma^2}\right) \quad (10)$$

$\text{map}$  denotes the 3D voxel maps, and  $\sigma$  is the standard deviation of measurement error in the LRF as determined experimentally.

With  $d(\cdot)$  as a function to acquire the average minimum distance between 3D maps and LRF measurement results, and  $N_t$  as the number of measurement points with LRF at time  $t$ , the following equation is established:

$$d(\text{map}, z_t, x_t) = \frac{1}{N_t} \sum_{n=1}^{N_t} \min \| \text{map} - f(z_{t,n}, x_t) \|^2 \quad (11)$$

where  $f(\cdot)$  is a function to convert LRF measurement results to coordinates on 3D voxel maps using the state vector  $x_t$  for the measured position and attitude. For this conversion, state vectors are first extended to 6-DOF, as stated in the preceding section, so that LRF measurement results with LRF can be converted to coordinates on voxel maps with the 3D position and attitude taken into consideration.

Note that the measurement probabilities  $p(z_t|x_t)$  become maximum when the distance in Eq. (11) is minimum. In this situation, the LRF measurement results completely match the 3D environment maps.

## VII. ACTUAL ENVIRONMENT TESTING AND PRECISION EVALUATION

### A. Experimental Environments and Methods

We conducted tests to evaluate our proposed method for position and attitude estimation using environmental 3D point cloud data. Fig. 7 shows the front-wheel driven, four-wheeled mobile robot we used in tests. It has no suspensions, has odometers on its wheels, has a one-axis MEMS gyroscope as an orientation (yaw angle) sensor, and has an LRF (PLS-101, SICK Inc.) installed parallel to the road surface to estimate the position and attitude.

We evaluated the precision for the estimated position and attitude using a dual-frequency GPS receiver and FOG to



measure the reference position and attitude. The results for the estimated position and attitude using 3D point clouds in our proposed method were compared to the true position and attitude acquired through post-analysis by carrier-phase DGPS/INS navigation.

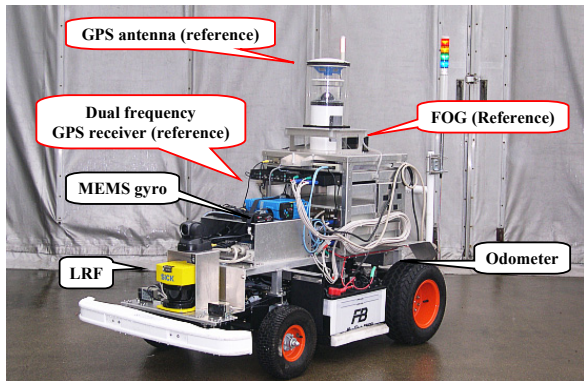


Fig. 7 Localization experiment robot configuration.

Fig. 8 shows the testing environments. Estimations of the position and attitude were carried out using a manually driven mobile robot running along the route in  $100\text{ m} \times 100\text{ m}$  environments (red solid line in Fig. 8). The total run distance was approximately 500 m at an average velocity of approximately 3.6 km/h. The position and attitude were estimated online at an acquisition frequency of 5 Hz with an LRF using a PC (Core2Duo 2.5 GHz) on the mobile robot.

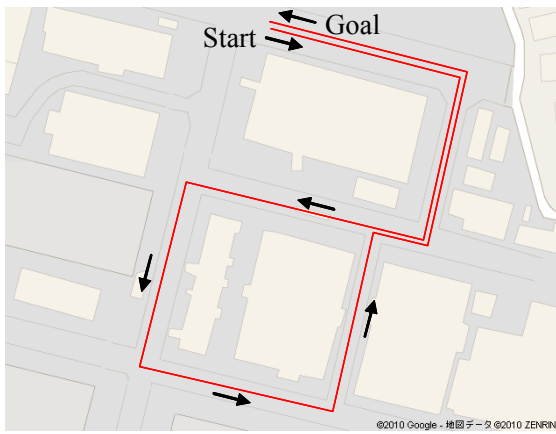


Fig. 8 Experimental environment and planned route.

### B. Experimental Results

Fig. 9 shows the run trajectories representing the position estimation results against an orthochromatic background of 3D point cloud data as measured with MMS. The red lines in Fig. 9 are trajectories determined using carrier-phase DGPS/INS navigation. The blue lines are estimation results using DR only. DGPS/INS navigation presented FIX-solutions of the carrier-phase DGPS for almost all of the area, indicating that its positioning precision is within a few centimeters or sufficiently adequate to serve as a reference.

Estimation results with DR show that due to encoder, gyroscope drift, and scale-factor errors in the sloping road surfaces, the estimation precision deteriorates over time and significantly deviates from the run route.

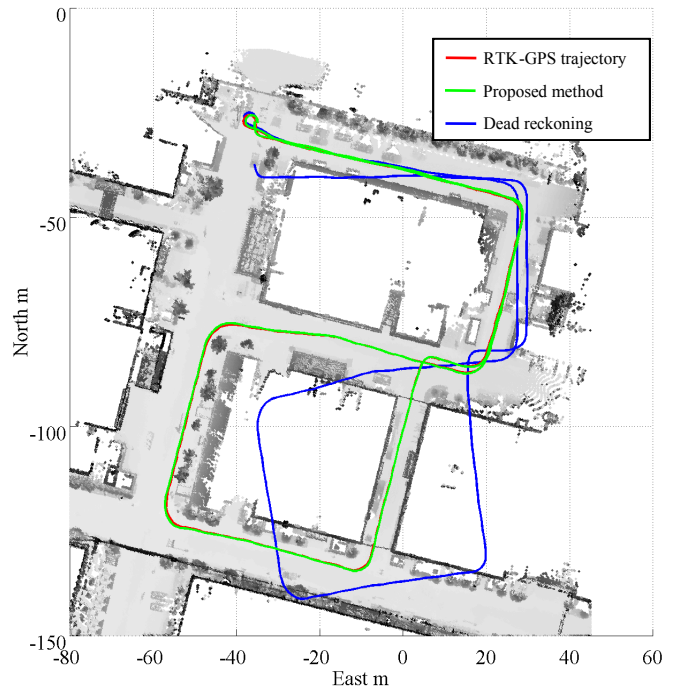


Fig. 9 Position estimated by our proposed method.

The position estimation for our proposed method using particle filters (green lines) resulted in run trajectories nearly identical to the DGPS/INS reference trajectories, which indicated that the accumulated DR error was corrected.

After the above evaluations, we evaluated the position and attitude errors estimated by our proposed method versus the true position and attitude measurement results from carrier-phase DGPS/INS navigation. Fig. 10 shows the time-series position distance errors for DR and our proposed method compared to the true values. Fig. 11 shows the time-series yaw-angular error for DR and our proposed method compared to the true values. Our proposed method was fairly accurate, with a position distance error maintained within 0.5 m and reasonably high precision when estimating the orientation.

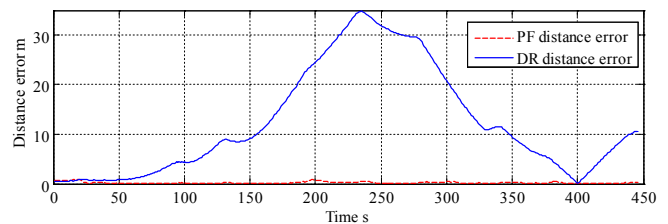


Fig. 10 Comparison with distance error.

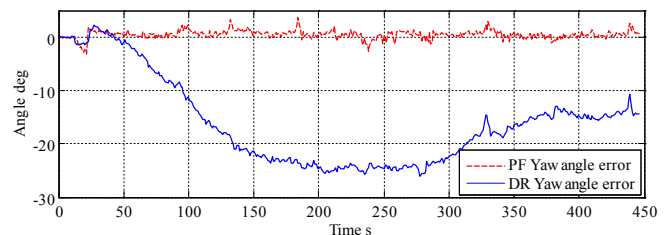


Fig. 11 Comparison to yaw angle error.

Fig. 12 shows the histograms for the distance and yaw angle errors in our proposed method compared to the true values. For the position estimation, the distance error (DRMS) versus the true value was 0.21 m, and the maximum distance error was 0.94 m. For the yaw angle estimation, the average error was  $0.51^\circ$ , and the standard deviation ( $1\sigma$ ) was  $0.78^\circ$ . These results show that our proposed method effectively estimates position and attitude with high precision.

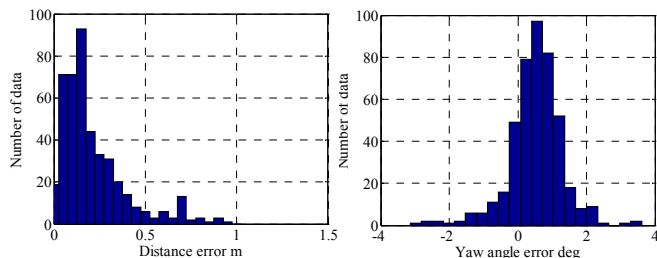


Fig. 12 Distance error histogram.

Fig. 13 shows the roll and pitch angles estimated by our proposed method in experimental environments. To evaluate the effectiveness of our proposed method in estimating 6-DOF position and attitude, we conducted a comparison based on the final estimation results for attitude through particle filters between two cases: when the 2D position and orientation are extended to the 6-DOF position and attitude, and when such extension is not applied.

The pitch angles changed as much as  $\pm 2^\circ$  due to road surface irregularities in the experimental environments. We did not use these roll or pitch angles but estimated positions by matching LRF measurement results to maps using particle filters in post-processing.

Compared to estimated position without extending 2D position and attitude to 3D versus true values, the distance error against true values (DRMS) increased from 0.21 m to 0.30 m, and the maximum distance error increased from 0.94 m to 1.41 m. This shows that our proposed method effectively improves the precision when estimating the position and attitude by extending 2D to 3D using 3D voxel maps of outdoor environments with irregularities.

The experiments showed the feasibility of high-precision position and attitude estimation in outdoor environments with simple sensor configurations using environmental 3D point clouds but no GPS.

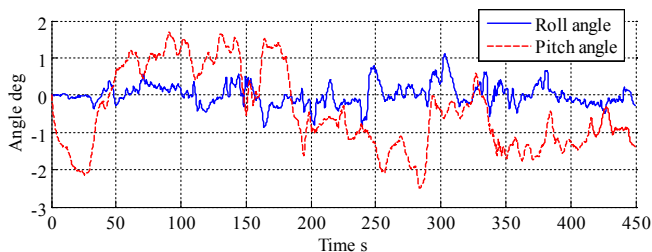


Fig. 13 Roll and pitch angle estimation results.

## VIII. CONCLUSIONS

In this paper, we have described how to estimate the position and attitude of mobile robots in outdoor environments by using environmental 3D point cloud data. We have quantized 3D point cloud data using MMS by voting the data points into voxel space. We have extended the 2D position and orientation to 3D using 3D point clouds, under the assumption that the mobile robot remains in continuous contact with the road surface. We have estimated the position and attitude of mobile robots using particle filters on the basis of the likelihood of their positions, which were calculated by matching LRF measurement results to 3D point cloud data measured using MMS. We have confirmed through run test comparisons in outdoor environments with carrier-phase GPS/INS navigation that we can determine the position of mobile robots within 30 cm without using GPS and we can reduce the errors due to sloping road surfaces or DR with 3D voxel map.

## REFERENCES

- [1] Sebastian Thrun, Wolfram Burgard, and Dieter Fox, "Probabilistic Robotics," The MIT Press, 2005.
- [2] F. Dellaert, et al., "Monte Carlo Localization for Mobile Robots," In *Proc. of IEEE ICRA*, pp. 1322–1328, 1999.
- [3] Feng Lu, and Evangelos Miliotis, "Robot Pose Estimation in Unknown Environments by Matching 2D Range Scans," *J. of Intelligent and Robotic Systems*, Vol.18, No. 3, pp. 249–275, 1997.
- [4] Dieter Fox, et al., "Monte Carlo Localization: Efficient Position Estimation for Mobile Robots," In *Proc. of AAAI*, pp. 343–349, 1999.
- [5] Jun-ichi Meguro, et al., "Autonomous Mobile Surveillance System based on RTK-GPS in Urban Canyons," *Journal of Robotics and Mechatronics*, No.17, Vol. 2, pp. 218–225, 2005.
- [6] Rui Hirokawa et al., "An Efficient UKF Based GPS/INS Augmented by Local Landmark Update," *Proc. ION GNSS*, pp. 127–134, 2007.
- [7] S. Thrun, et al., "Stanley, the robot that won the DARPA Grand Challenge," *Journal of Field Robotics*, Vol.23, No.9, pp.661–692, 2006.
- [8] D. Barber, et al., "Geometric validation of a ground-based mobile laser scanning system," *ISPRS Journal of Photogrammetry and Remote Sensing*, Vol. 63, No. 1, pp. 128–141, 2008.
- [9] Kiichiro Ishikawa, et al., "A Mobile Mapping System for Precise Road Line Localization Using Single Camera and 3D Road Model," *Journal of Robotics and Mechatronics*, Vol. 19, No. 2, pp. 174–180, 2007.
- [10] Kremer, J., Hunter, G., "Performance of the StreetMapper Mobile LIDAR Mapping System in Real World Projects," *Photogrammetric Week '07*, pp. 215–225, 2007.
- [11] Lingemann, K., et al., "High-speed laser localization for mobile robots," *Robotics and Autonomous Systems*, Vol.51, pp. 275–296, 2005.
- [12] A. Nüchter, et al. "6D SLAM - 3D Mapping Outdoor Environments, Quantitative Performance Evaluation of Robotic and Intelligent Systems," *Journal of Field Robotics*, Vol.24, No.8, pp.699–722, 2007.
- [13] A. Davison, et al., "Monoslam: Real-time single camera slam," *IEEE Trans. on Pattern Analysis and Machine Intelligence*, Vol. 29, No. 6, pp. 1052–1067, 2007.
- [14] S. Thrun, et al., "Robust Monte Carlo Localization for Mobile Robots," *Artificial Intelligence Journal*, Vol.128, No.1–2, pp. 99–141, 2001.
- [15] Rainer Ku" mmerle, et al. "Monte Carlo Localization in Outdoor Terrains Using Multilevel Surface Maps," *Journal of Field Robotics*, Vol. 25, No. 6-7, pp.346-359, 2008.
- [16] K. Lingemann, et al., "High-speed laser localization for mobile robots," *J. of Robotics and Autonomous Systems*, Vol. 51, No.4, pp.275-296, 2005.
- [17] Olson, E.B., "Real-time correlative scan matching," *Proc. of IEEE Int. Conference on Robotics and Automation*, pp.4387–4393, 2009.
- [18] Tom Duckett, et al., "Mobile Robot Self-Localisation Using Occupancy Histograms and A Mixture of Gaussian Location Hypotheses," *J. Robotics and Autonomous Systems*, Vol.34, No. 2-3, pp. 119-130, 2001.